Top Curr Chem (Z) (2017) 375:60
DOI 10.1007/s41061-017-0145-4

REVIEW

Construction of Polyarylenes with Various Structural Features via Bergman Cyclization Polymerization

Youfu Wang[1] · Shudan Chen[1] · Aiguo Hu[1]

Received: 24 November 2016 / Accepted: 6 May 2017 / Published online: 22 May 2017

Abstract Synthetic polymer chemistry is a fundamental part of polymer science, and highly efficient polymerization reactions are essential for the synthesis of high-performance polymers. Development of new synthetic methods for emerging polymer science is of great importance in this regard. Bergman cyclization is a chemical process in which highly reactive aryl diradicals form from enediyne precursors, having a strong impact in a number of fields including pharmaceutics, synthetic chemistry, and materials science. Diradical intermediates stemming from enediynes can cause DNA cleavage under physiological conditions, leading to the strong cytotoxicity of many naturally occurring enediyne antibiotics. Meanwhile, diradical intermediates can quickly couple with each other to construct polyarylenes, providing a novel method to synthesize these conjugated polymers with the advantages of facile and catalyst-free operation, high efficiency, and tailored structure. Moreover, conjugated polymers generated by Bergman cyclization exhibit many remarkable properties, such as excellent thermal stability and good solubility and processability, enabling their further processing into carbon-rich materials. This review presents a brief overview of the trajectory of Bergman cyclization in polymer science, followed by an introduction to research advances, mainly from our group, in developing polymerization methods based on Bergman cyclization, taking advantages of its catalyst-free, byproduct-free, in situ polymerization mechanism to synthesize new polymeric materials with various structures and morphologies. These synthetic strategies include fabrication of rod-like polymers with polyester,

This article is part of the Topical Collection "Polymer Synthesis Based on Triple-bond Building Blocks"; edited by Ben Zhong Tang, Rongrong Hu.

✉ Aiguo Hu
hagmhsn@ecust.edu.cn

[1] Shanghai Key Laboratory of Advanced Polymeric Materials, School of Materials Science and Engineering, East China University of Science and Technology, Shanghai 200237, China

dendrimer, and chiral imide side chains, functionalization of carbon nanomaterials by surface-grafting conjugated polymers, formation of nanoparticles by intramolecular collapse of single polymer chains, and construction of carbon nanomembranes on the external and internal surface of inorganic nanomaterials. These polymers with novel structural features have been used in a variety of fields, such as energy transformation, energy storage, catalyst support, and fluorescent detection. Finally, the outlook for future developments of Bergman cyclization in polymer science is presented.

Keywords Bergman cyclization · In situ polymerization · Enediynes · Conjugated polymers · Two-dimensional polymers

Abbreviations

APTES	*N*-Aminopropyltriethoxysilane
BET	Brunauer–Emmett–Teller
BODA	Bis-*ortho*-diynylarene
C-dots or CDs	Carbon quantum dots
CL	ε-Caprolactone
CMPs	Conjugated microporous polymers
CNMs	Carbon nanomembranes
CNs	Cyclo-1,4-naphthylenes
CV	Cyclic voltammetry
DMA	Dynamic mechanical spectroscopy
DMF	*N*,*N*-Dimethylformamide
DNHD	*cis*-1,6-Di-2-naphthylhex-3-ene-1,5-diyne
ECs	Electrochemical capacitors
EDLCs	Electrical double-layer capacitors
EDY	Enediyne
FARs	Fused aromatic rings
GPC	Gel permeation chromatography
HOMO	Highest occupied molecular orbital
LUMO	Lowest unoccupied molecular orbital
MMA	Methyl methacrylate
MWNTs	Multiwalled carbon nanotubes
NMP	*N*-Methylpyrrolidone
PAA	Poly(acrylic acid)
PBzA	Poly(benzyl acrylate)
PDI	Polydispersity index
PEG	Polyethylene glycol
PL	Photoluminescence
PLA	Polylactic acid
PMA	Poly(methyl acrylate)
PNs	Polynaphthalenes
PPPs	Poly(*p*-phenylene)s
PS	Polystyrene

QDs	Quantum dots
QY	Quantum yield
SAED	Selected-area electron diffraction
SAMs	Self-assembled monolayers
SCMPs	Soluble conjugated microporous polymers
SCNPs	Single-chain polymer nanoparticles
SERS	Surface-enhanced Raman scattering
SS-CNMs	Silica-supported carbon nanomembranes
STM	Scanning tunneling microscopy
TBAF	Tetrabutylammonium fluoride
TEM	Transmission electron microscopy
TMS	Trimethylsilyl

1 Introduction

Developments in modern synthetic organic chemistry, taking advantage of rational molecular design and structural control at molecular level, have enabled preparation of novel polymers and nanostructured materials. Such highly efficient organic reactions are recognized as forming an important toolbox for construction of polymeric materials for use in a wide range of fields. Considering its broad scope and simple operation, Bergman cyclization for intramolecular cyclization of enediyne compounds has been extensively investigated for application in synthetic chemistry, pharmaceutical chemistry, and polymer science.

The seminal work concerning Bergman cyclization was reported by Bergman et al. in the early 1970s [1, 2]. They found that *cis*-1,5-hexadiyn-3-ene underwent exclusively thermal rearrangement to generate a 1,4-didehydrobenzene intermediate which could easily be trapped by external reagents to yield benzene derivatives (Fig. 1a). However, Bergman's research did not receive much attention until the late 1980s, when the enediyne-type core structures of many naturally occurring antibiotics, such as calicheamicin [3, 4], dynemicin A [5], esperamicin A_1 [6, 7], and kedarcidin chromophore [8] were reported. The enediyne "warheads" of these antibiotics are readily triggered in vivo to generate 1,4-phenylene diradicals, which further cause DNA cleavage or crosslinking. This strong cytotoxicity arising from Bergman cyclization motivated a flurry of activity on synthesis of biosimilar enediyne compounds, especially hetero- and metalloenediynes, for potential application in antitumor medicines [9–12].

The therapeutic applications of these enediyne antitumor antibiotics also triggered a series of research efforts in connection with enediyne chemistry, including quantum-chemical theory, thermodynamics, and kinetics studies of Bergman cyclization [13]. Based on these studies, it was determined that the activation barrier for Bergman cyclization is influenced by three dominant factors: (1) the proximity effect [14], stating that the critical distance between the two enediyne carbon atoms forming the new bond should be in the range of 3.31–3.20 Å for spontaneous Bergman cyclization at physiological temperature; (2) molecular-strain differences [15, 16], leading to significant activation of some cyclic

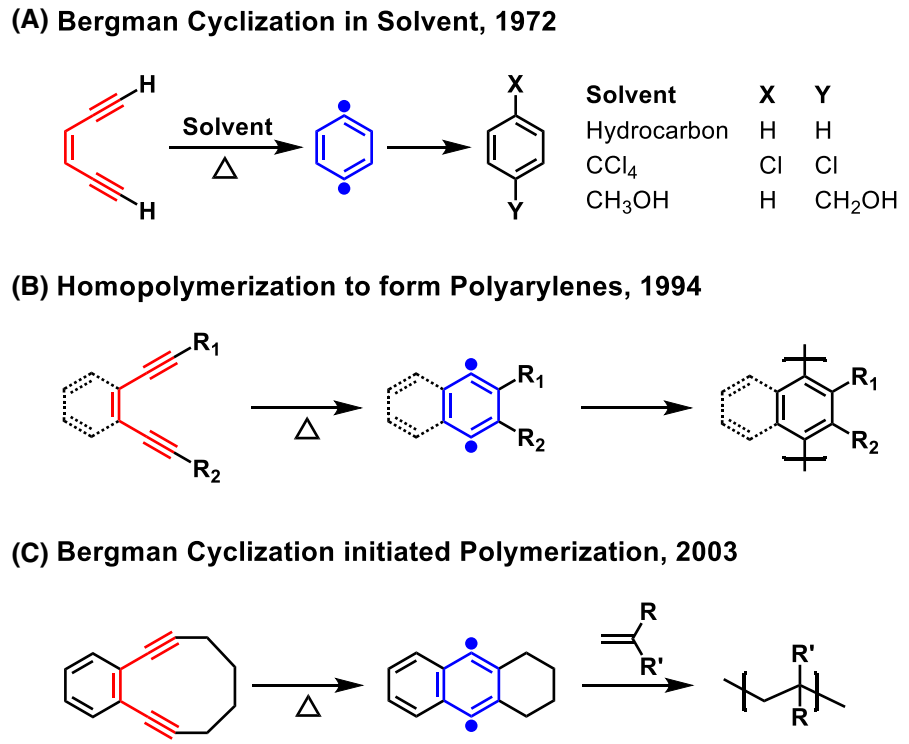

Fig. 1 Prototypical EDY structure and Bergman cyclization in solution (**a**) and development of Bergman cyclization in polymer chemistry. The diradical generated from Bergman cyclization acts as monomer for homopolymerization to form polyarylenes (**b**) or as initiator to polymerize vinyl monomers (**c**)

enediynes; and (3) electronic effects [17], influencing the stability of the rearranged enediyne, the transition state, and the diradical species that is produced. In general, all these factors act synergistically to drive the process of diradical generation at physiologically relevant temperature (namely the onset temperature), therefore playing an instrumental role in the development of design strategies for enediynes, especially in the case of thermally triggered Bergman cyclization. Besides heat, Bergman cyclization can also be triggered by other stimuli such as ultraviolet (UV) radiation, acidic conditions, and organometallic catalysts [11, 18–21].

Bergman cyclization has also proven to be a promising tool in polymer and materials science. Tour et al. [22] first carried out radical polymerization via thermally triggered Bergman cyclization to obtain conjugated aromatic polymers such as poly(*p*-phenylene)s (PPPs) and polynaphthalenes (PNs) in 1994 (Fig. 1b), thereby highlighting Bergman cyclization as a new synthetic tool for polymers or other materials. Smith et al. [23, 24] subsequently used Bergman cyclization of bis(*o*-diynylarene) (BODA) to form branched oligomers at 210 °C, which could either react with carbon nano-onions to improve their solubility, or be carbonized to generate glassy carbon. Moore et al. [25, 26] used diradicals generated via Bergman cyclization to initiate radical polymerization of a variety of vinyl monomers

(Fig. 1c). The results showed that the diradicals tend to terminate intramolecularly to produce oligomeric byproducts. The high-molecular-weight polymer produced in the diradical-initiated system could only be expected to result from the monoradical formed after the diradicals undergo chain transfer with a monomer, polymer, or other available chain-transfer agent. Following this line, Barner-Kowollik et al. [27] reported the first reversible addition–fragmentation chain transfer (RAFT) polymerization of methyl methacrylate initiated by an aryl diradical, employing a cyclic enediyne as diradical source and cyanoisopropyl dithiobenzoate (CPDB) as RAFT agent. They successfully obtained very high molecular weights up to almost 400 kDa with narrow polydispersity under mild reaction conditions.

These studies established ideal platforms for the preparation of polymers and carbon materials with unique electronic and photovoltaic properties as well as excellent thermal stability and processability, which aroused our curiosity to further explore this field. Therefore, considerable research has been conducted in our group to prepare novel functional materials and develop new synthetic methods based on Bergman cyclization. We have successfully prepared a variety of structurally unique materials, such as brushed polymers, chiral conjugated polymers, nanoparticles, carbon nanomembranes, and nanodevices in recent years. This review summarizes our most recent research results on this topic together with some closely related work from other groups, hoping to attract more attention to this appealing area.

2 Synthesis of Linear Conjugated Polymers

Bergman cyclization is especially attractive for the synthesis of linear conjugated polymers, as it is a simple, byproduct-free synthetic route involving one component with no strict requirements in terms of catalysts or additives. Taking advantage of the designable structure of enediynes, it is very easy to modulate the reaction conditions and variegate the structure, performance, and application of the conjugated polymers. Although still in its infancy, Bergman cyclization has already appeared as a valuable tool in polymer chemistry, where it is applied in a twofold way: (1) The highly reactive *p*-benzynes generated by Bergman cyclization can undergo homopolymerization, acting as symmetrical bifunctional monomers; (2) The highly reactive radicals at the chain ends of the conjugated polymers can also be used to covalently modify carbon materials to improve their solubility in organic solvents [23, 28].

2.1 Linear Conjugated Backbones with Various Side Chains

In the case of homopolymerization, a variety of rigid conjugated polymers with excellent thermochemical properties can be obtained through Bergman cyclization [22, 24, 29]. Attempting to resolve the fundamental principles in this field, we published the first report on the on-surface formation of one-dimensional polyphenylene chains through Bergman cyclization on a Cu(110) surface [30].

Initially, an enediyne compound (DNHD) terminated with two naphthyl substituents was designed as the monomer. After deposition of DNHD molecules on Cu(110) substrate held at −103 °C (170 K), heart-shaped molecules with two

elliptical lobes and one round protrusion were distributed in an isolated manner on the substrate, as illustrated by scanning tunneling microscopy (STM). The heart-shaped motifs disappeared and dispersed one-dimensional chains grew on the surface of the substrate (Fig. 2) when the sample was annealed to 127 °C (400 K). It is plausible to deduce that on-surface formation of one-dimensional (1D) polyphenylene through Bergman cyclization of the enediyne precursor was successfully achieved. This result was also validated by comparison with the STM image of the monomeric product of Bergman cyclization of DNHD via ex situ synthesis. These findings demonstrated that Bergman cyclization could be a promising tool for construction of molecular nanostructures containing conjugated backbones with submolecular precision, which would aid design of molecular nanodevices with engineered chemical and electronic properties.

Unfortunately, conjugated polymers such as PPPs and PNs obtained by Bergman cyclization are insoluble in common solvents, as reported by Tour et al. [22]. Introducing a pendant moiety onto the conjugated polymer to form a polymer brush [31] is a generic way to improve the solubility and modify the electrical properties of these rod-like polymers. We successfully synthesized "rod-coil" brush conjugated polymers via the combination of ring-opening polymerization (ROP) and Bergman cyclization polymerization [32]. As shown in Fig. 3, the enediyne compound **2** was synthesized initially and the poly(ε-caprolactone) (PCL) **3** chain was subsequently installed via ring-opening polymerization of caprolactone. After protection of the terminal hydroxyl group with acetylation reaction and deprotection of the TMS group, the PCL **4** was transferred into a refluxing diphenyl ether bath

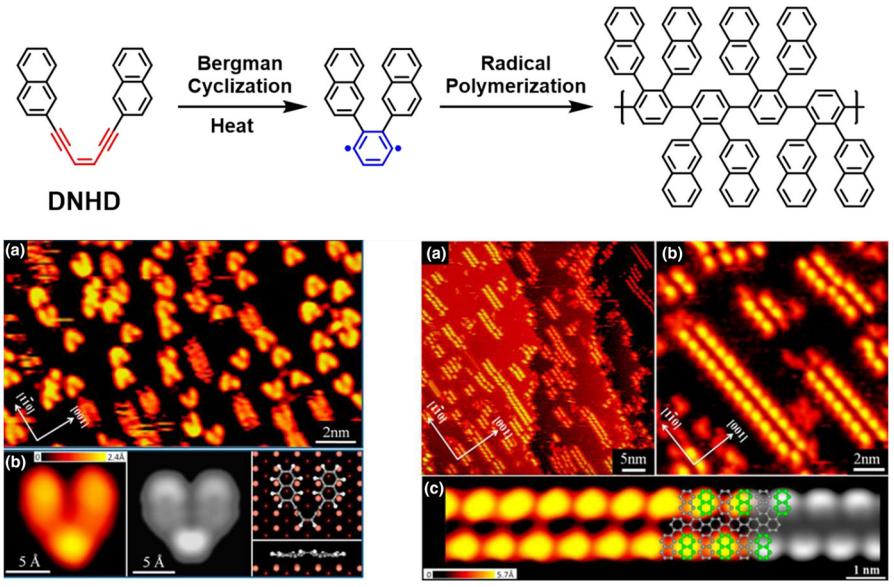

Fig. 2 (*Top*) Mechanism of Bergman cyclization and radical polymerization of DNHD. (*Bottom*) Large-scale and close-up STM images of DNHD molecules and the obtained polyarylenes on the surface of single-crystalline copper. Reproduced from [30] with permission from ACS

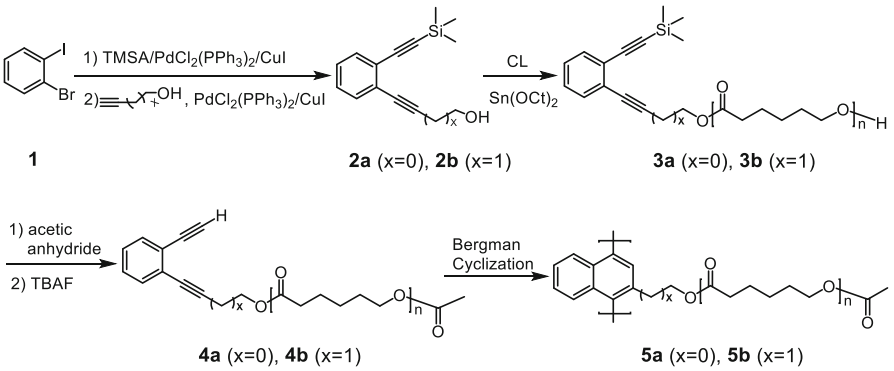

Fig. 3 Synthetic route for polymer brush [32]

(259 °C) to undergo thermal Bergman cyclization for 6 h to produce the polymer brush **5**. It should be noted that the acetylation reaction is an indispensable step, because hydroxyl groups may quench the free radicals generated by thermal Bergman cyclization. Occurrence of thermal Bergman cyclization was proven by recording the infrared (IR) spectrum, from which two adsorption peaks at around 2180 and 2230 cm^{-1}, representative of internal and terminal triple bonds, disappeared after the heating treatment. The reaction was further supported by UV–Vis spectroscopy, which showed strong adsorption tailing up from 237, 263, and 278 nm to 450 nm without a notable difference between two types of macromonomer (**3a**, **b**), indicating formation of a long conjugated system subsequent to Bergman cyclization. GPC analysis revealed broad molecular weight dispersion, which was due to the step-growth nature of the coupling reaction of the diradicals generated via Bergman cyclization [22]. Interestingly, the conjugated brush polymers showed high molecular weights up to 106 kDa. The flexibility of the PCL side chain allowed a solution nuclear magnetic resonance (NMR) spectrum to be obtained after Bergman cyclization, revealing two new sets of peaks at around 6.6 and 8.1 ppm, confirming that the rigid backbone of the brush polymers was formed of copolymers of indenylenemethylene and naphthalene, previously considered to possibly have been formed by Johnson et al. [33].

Dendronized polymers with rigid conjugated backbones were synthesized through a similar process [34]. Two generations of Fréchet-type dendrimers were conically incorporated with compound **2b**, followed by deprotection of the TMS group and Bergman cyclization to form the dendronized polymers **10** and **11** (Fig. 4). IR, ^1H NMR, and UV–Vis spectra showed disappearance of the acetylene groups and formation of the conjugated backbone, which can be rationalized as random copolymers of naphthalene and indenylenemethylene as well. GPC revealed a broad molecular weight distribution, and the degree of polymerization (DP) of **10** and **11** was thus calculated to be 3624 and 83, respectively. The latter result clearly indicates that an increase in the generation of dendritic wedges suppresses the polymerization of diradicals generated from Bergman cyclization.

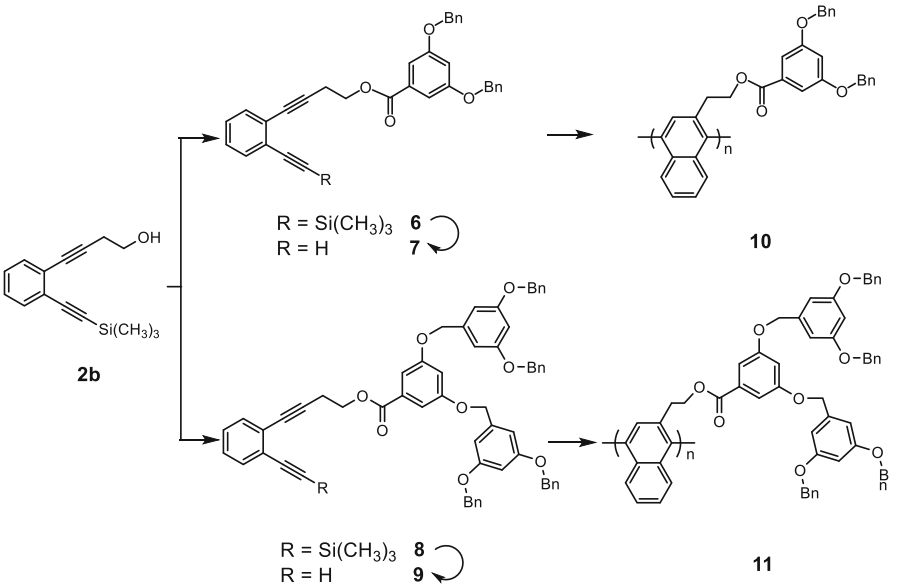

Fig. 4 Synthetic route for dendronized polymers [34]

Helical chirality endows PNs with excellent resistance to racemization, making them potential candidates for application in asymmetric catalysis and enantioselective separation. This led us to conceive the idea of incorporating chiral imides into a series of polymer brushes [35]. The enediynes containing the chiral imides were synthesized through treatment of 4,5-dibromophthalic acid with a chiral amine, (*R*)-(+)-α-methylbenzylamine, and subsequent incorporation of long-chain alkyl or alkoxyl groups via Sonogashira coupling reaction. The soluble chiral

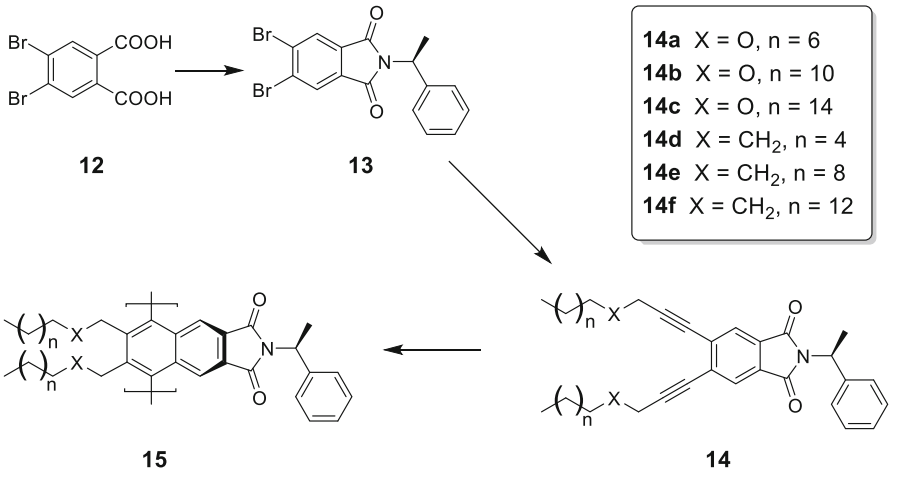

Fig. 5 Synthetic route for chiral conjugated polymers [35]

conjugated polymers **15** were obtained through Bergman cyclization (Fig. 5) of these chiral enediyne compounds. Unfortunately, after thermal treatment at 259 °C, only featureless circular dichroism (CD) spectra were obtained for the polymers (**15a–c**), indicative of a racemic mixture due to the harsh reaction conditions. Changing the alkyloxy propargyl groups to simple long alkynyl chains resulted in the observation of a dramatic drop of the onset temperature from ~200 to ~130 °C. When Bergman cyclizations were conducted in a refluxing bath of *N*,*N*-dimethylacetamide (166 °C), almost mirror-imaged CD patterns were observed for the polymers obtained from *R*-**14d** and *S*-**14d** (Fig. 6). Furthermore, after removal of the chiral directing group, the peak corresponding to the chiral imide unit completely disappeared, whereas a weak peak at 270 nm remained, and could be rationalized based on the chirality of the main chain.

Enlightened by this work, we synthesized a family of maleimide-based enediynes. The two adjacent carbonyl groups in the maleimide moiety serve to lower the energy barrier for Bergman cyclization, permitting the reaction to take place at an even lower temperature (130–160 °C) [36]. This result directed us to choose compound **16** as the precursor to prepare chiral conjugated polymers due to its relatively low onset temperature of 135 °C (Fig. 7) [37]. Interestingly, the polymer prepared in bulk showed a new set of signals in the CD spectra in the range of 400–500 nm, which did not exist in the CD spectrum of the reference compound, further corroborating the existence of main-chain chirality in the conjugated polymers (Fig. 8).

2.2 Grafting Linear Conjugated Polymers onto Carbon Nanomaterials

Aside from its applications for the synthesis of linear conjugated polymers, Bergman cyclization has also been used to covalently modify carbon nanomaterials via radical addition to sp^2 carbons and thus improve their solubility and dispersibility in organic solvents.

Based on our previous work, we utilized enediyne-containing compounds **18** as precursors to modify multiwalled carbon nanotubes (MWNTs) followed by

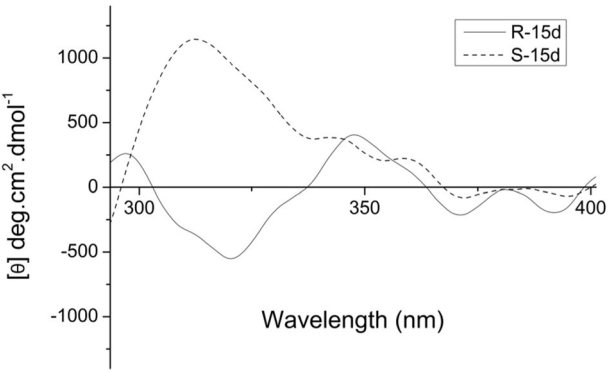

Fig. 6 CD spectra of chiral conjugated polymers *R*-**15d** (*solid line*) and *S*-**15d** (*dotted line*) [35]

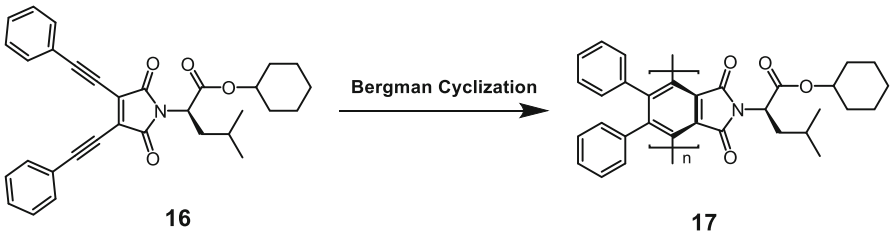

Fig. 7 Synthetic route for chiral conjugated polymers from enediynes with low onset temperature [37]

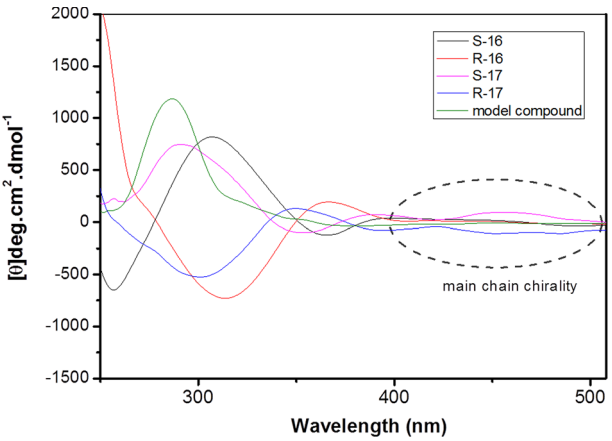

Fig. 8 CD spectra of chiral enediyne compounds (*S*-**16**, *R*-**16**), conjugated polymers (*S*-**17**, *R*-**17**), and model compound [37]

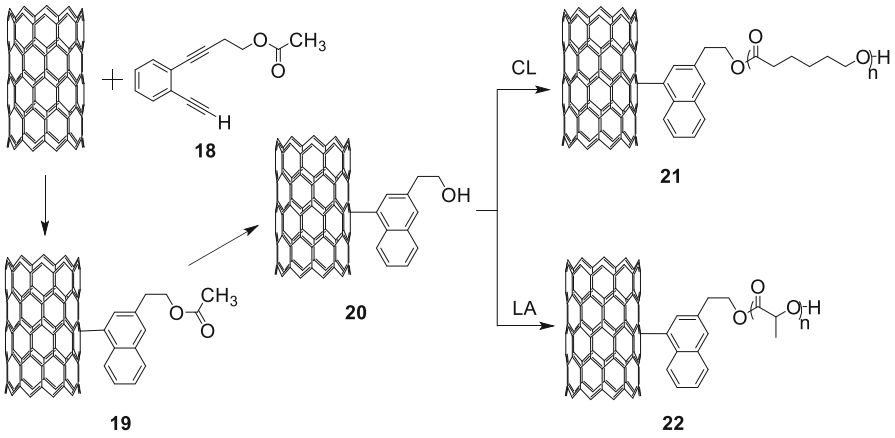

Fig. 9 Surface functionalization of MWNTs and ring-opening polymerization of CL and lactic acid (LA) [38]

attachment of polyester chains (PCL and PLA) via a "grafting from" strategy (Fig. 9) [38]. Due to exfoliation of the bundles of MWNTs by the polyesters grafted onto the sidewall, the functionalized MWNTs can be easily dispersed in

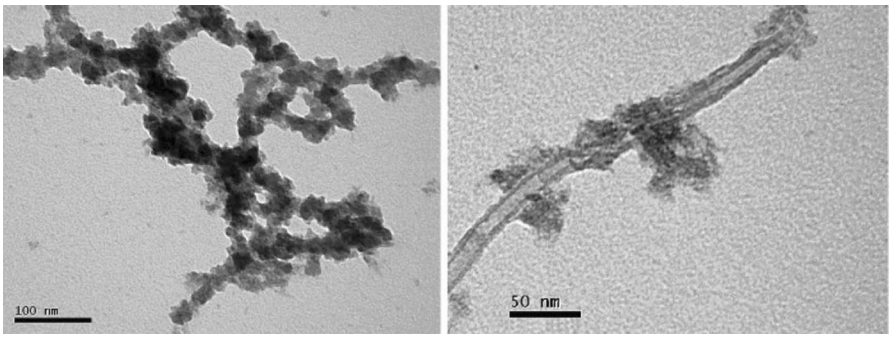

Fig. 10 TEM images of MWNTs-PCL (**21**) (*left*) and MWNTs-PLA (**22**) (*right*). Reproduced from [38] with permission from Wiley–VCH

many common organic solvents such as *N*-methylpyrrolidone, CH_2Cl_2, *N*,*N*-dimethylformamide (DMF), and tetrahydrofuran (THF). The black homogeneous solutions of functionalized MWNTs formed in these solvents are stable indefinitely. Further substantiation of the functionalized MWNTs was provided by TEM images, which showed a substantial amount of amorphous organic layer on the surface of MWNTs (Fig. 10). Additional evidence for the effectiveness of this functionalization method was provided by the mechanical and thermal properties of the composite polymer fibers prepared by electrospinning with PCL. The MWNTs were well distributed in the PCL fibers, with their axes parallel to the direction of the PCL fibers. This axial arrangement proved to be the main factor enhancing the strength of the PCL fibers.

Dendrimer-containing enediynes **7** and **9** were also utilized for functionalization of MWNTs via a grafting-onto strategy. After this surface functionalization, the nanocomposites showed good solubility/dispersibility in common organic solvents as well as in polymer solutions. Compared with MWNTs-PCL and MWNTs-PLA, the dendrimer-functionalized MWCNTs revealed enhanced thermal stability [39].

Furthermore, we extended this work by introducing enediyne **7** and its analogs onto pristine graphene. Without the need for oxidation or pretreatment of graphene, the surface functionalization proceeded smoothly to graft conjugated polymers onto graphene through Bergman cyclization (Fig. 11) [40]. The modified graphene samples exhibited good solubility in many organic solvents and high electric conductivity when compressed into tablet form. The structural variability of enediyne molecules allows a wide range of functional groups to be attached onto pristine graphene under similar conditions, offering a new method for one-pot synthesis of graphene–polymer composite materials.

3 Synthesis of Polymeric Nanoparticles

With the development of "nano" chemistry, facile synthesis of molecules or particles of any possible size, morphology, and functionality is desirable; For example, single-molecule dendrimer synthesis provides access to particles up to

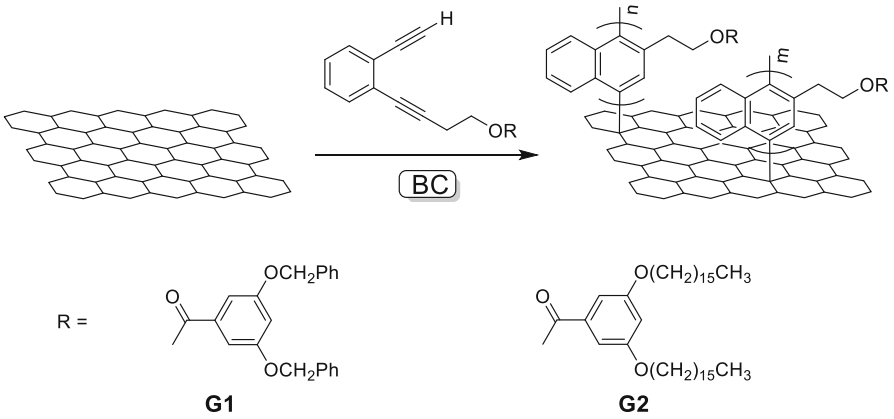

Fig. 11 Functionalization of pristine graphene with enediyne molecules [40]

approximately 5 nm in size [41], and self-assembly of amphiphiles or mini-emulsion polymerizations lead to particle constructs down to around 20 nm. However, particles in the size range of 5–20 nm have drawn significant interest in the past decade due to their diverse applications in catalysis, drug delivery systems [42, 43], light and energy harvesting [44], and nanoporous low-dielectric-constant materials for microelectronic applications [45]. Intramolecular collapse of single polymer chains represents a promising approach for this type of nanoparticle [46–48]. Since Mecerreyes et al. [45] first used a radical initiator to radically crosslink the pendent acrylate functionalities along a polycaprolactone or poly(methylmethacrylate) backbone under ultradilute conditions, development of a slow addition method has resulted in the ability to feasibly synthesize single-chain polymer nanoparticles (SCNPs) on a larger scale. To date, a variety of crosslinking methods have been used in SCNP synthesis, including high-temperature self-condensation of benzocyclobutene [46, 49], benzoxazines [50], and sulfonyl azides [51]. Click reactions, Glaser–Hay coupling of alkynes, and the tetrazine–norbornene reaction have also been employed for single polymer chain collapse [52]. Aside from these crosslinking methods, Bergman cyclization produces crosslinkable diradical intermediates under various conditions, which can afford advantages to facilitate preparation of polymeric nanoparticles, and further application for fabrication of size-controlled carbon dots and encapsulation of quantum dots is also available.

Two strategies have been used for synthesis of linear polymer precursors [53]: (1) copolymerization of enediyne-containing methacrylate with methyl methacrylate (MMA) through living radical polymerization (Fig. 12) and (2) attachment of the enediyne-containing alkyloxyamine compound to polymers (Fig. 13). After removal of the TMS protection group, the polymer was subjected to Bergman cyclization-mediated intramolecular chain collapse in hot diphenyl ether under ultradilute conditions or by continuous addition technique to produce polymeric nanoparticles. As expected, the apparent molecular weights were observed to drop significantly for all the systems after Bergman cyclization, implying formation of nanoparticles. This

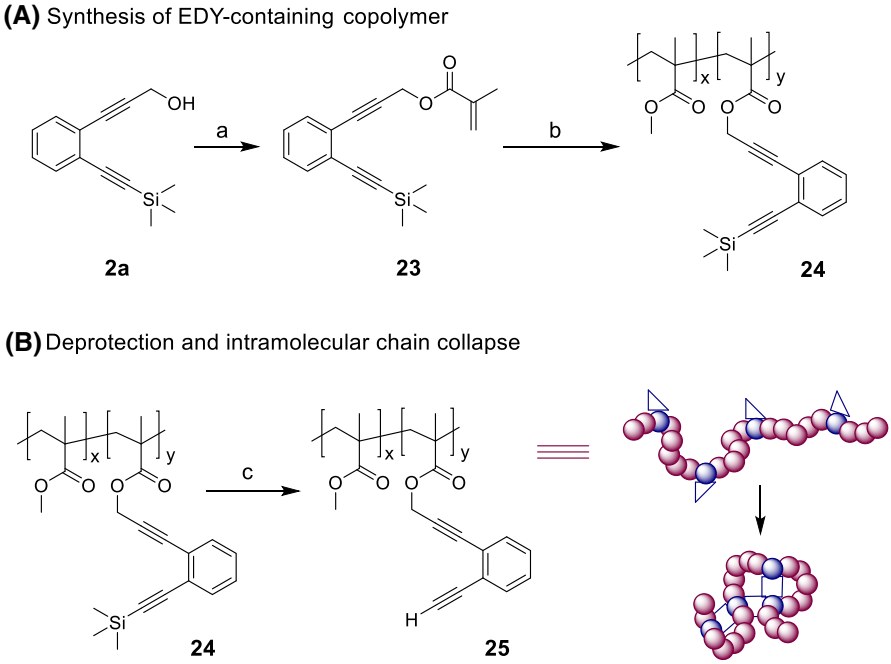

Fig. 12 Synthesis of polymer nanoparticles. Route 1: **a** methacrylic acid, N,N'-Dicyclohexylcarbodiimide, 4-dimethylaminopyridine, THF, RT, 60 %. **b** Ethyl-2-bromoisobutyrate, MMA (5–20 eq.), CuCl, pentamethyldiethylenetriamine (PMDETA), anisole, 80 °C. **c** TBAF, THF [53]

is quite a reasonable conclusion because the nanoparticles are much more compact after cross-linking, thus showing smaller hydrodynamic volume. In addition, no intermolecular cross-linking or chain-scission processes occurred, as GPC did not reveal a shoulder peak on either the high or low molecular weight side. The "tightness" of the polymeric nanoparticles is controllable by adjusting the enediyne content in the linear polymer precursors. This is not surprising because higher enediyne content results in a much more densely cross-linked network. The polymeric nanoparticles were well separated when spin-coated onto silicon wafer (Fig. 14). Assuming the particles to have the shape of half an ellipsoid on the flat surface, the diameters of the nanoparticles were calculated to be 4.7–8.7 nm, with an average of 6.36 nm. These ultrasmall nanoparticles were then used as sacrificial pore generators to fabricate low-*k* spin-on dielectrics.

As the reaction conditions (>200 °C) are considered harsh for most thermally sensitive polymers, such as poly(*t*-butyl acrylate), this may suppress the universality of Bergman cyclization for preparation of SCNPs; thus, phototriggered Bergman cyclization was also integrated with intramolecular chain collapse to yield nanoparticles with calculated diameter of $\sim$10 nm [54]. The enediyne motif was carefully designed to possess high photoreactivity, with the double bond locked in a methyl benzoate ring and the triple bonds substituted with phenyls. A few vinyl monomers were used to further verify its applicability, including methyl acrylate (MA), ethyl acrylate (EA), butyl acrylate (BA), and *tert*-butyl acrylate (*t*BA).

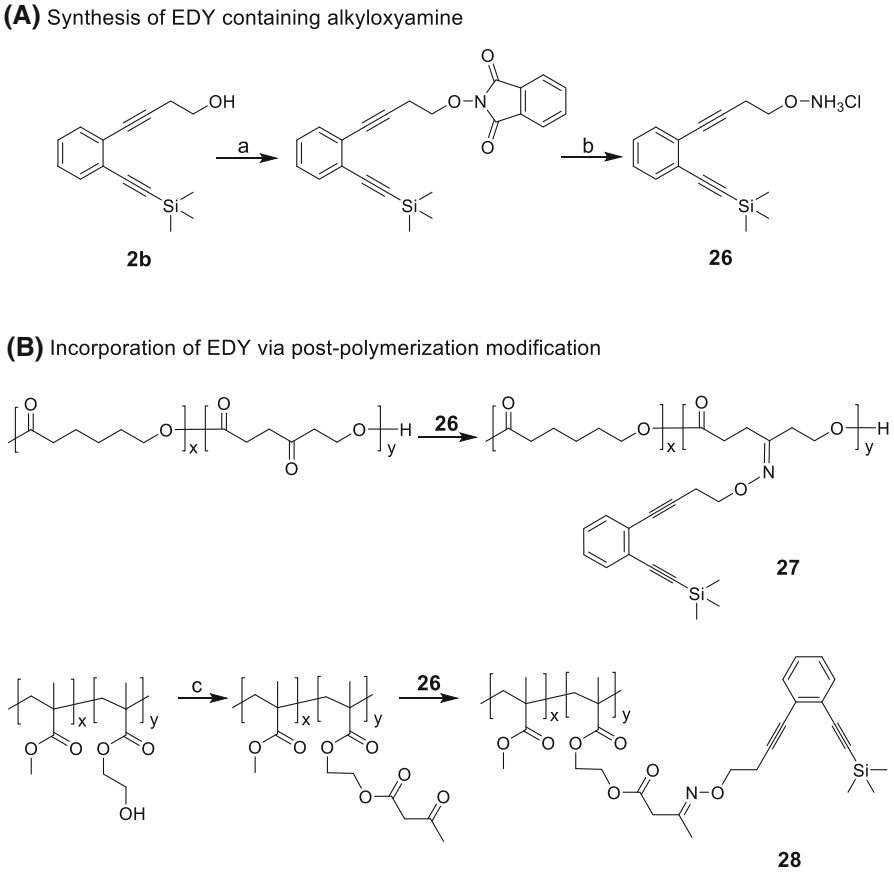

Fig. 13 Synthesis of polymer nanoparticles. Route 2: **a** Diisopropyl azodicarboxylate (DIAD), PPh_3, *N*-hydroxyphthalimide, THF, RT, 70 %. **b** hydrazine, Et_2O, RT, then HCl (aq.), 57 %. **c** diketene, Et_3N, CH_2Cl_2 [53]

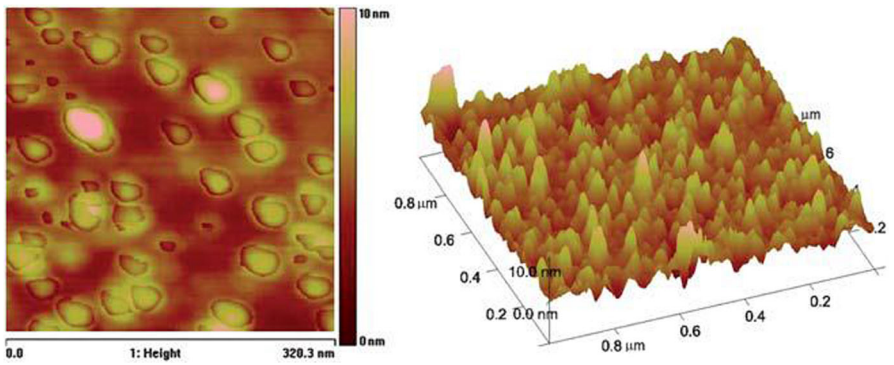

Fig. 14 Atomic force microscopy (AFM) images of polymer nanoparticles on silicon wafer. Reproduced from [53] with permission from RSC

The size-tunable SCNPs also served as ideal precursors for controllable fabrication of photoluminescent carbon quantum dots (C-dots) [55]. As shown in Fig. 15, the transesterification reaction between enediyne **2b** and poly(methyl acrylate) (PMA) was carried out to obtain the EDY-modified copolymer P(MA-r-EDY), followed by deprotection of TMS and Bergman cyclization. The precursor PMA nanoparticles were mixed with pure PMA and carbonized at 500 °C, thereby generating each C-dot from a single PMA nanoparticle. With this so-called bijective approach, the size of these C-dots could be tuned by varying the molecular weight of PMA and the molar fraction of the enediyne moiety in the copolymer. The composition and surface chemistry of these C-dots are controlled during carbonization and surface treatment. The photoluminescence mechanism of the C-dots was further investigated by fabricating three series of narrowly dispersed C-dots (CD 1-3) with average diameter of 4.5, 2.1, and 2.0 nm. After surface modification with a diamine-terminated polyethylene glycol (PEG_{2000N}), all the C-dots were found to produce effective and stable photoluminescence, as shown in Fig. 16 (only CD-1 and CD-2 are shown).

Different from the trends typically found in semiconductor quantum dots and C-dots prepared from graphitized materials, the optimal emission wavelength of these C-dots exhibits a red-shift as the size decreases. On the other hand, the PL spectra of the C-dots with reduced surface (treated with $NaBH_4$) exhibit a similar emission wavelength compared with their surface-oxidized counterparts under the same excitation wavelength, but the QY decreased significantly. Thus, we rationalized that the surface chemistry does not affect the energy gap of the C-dots

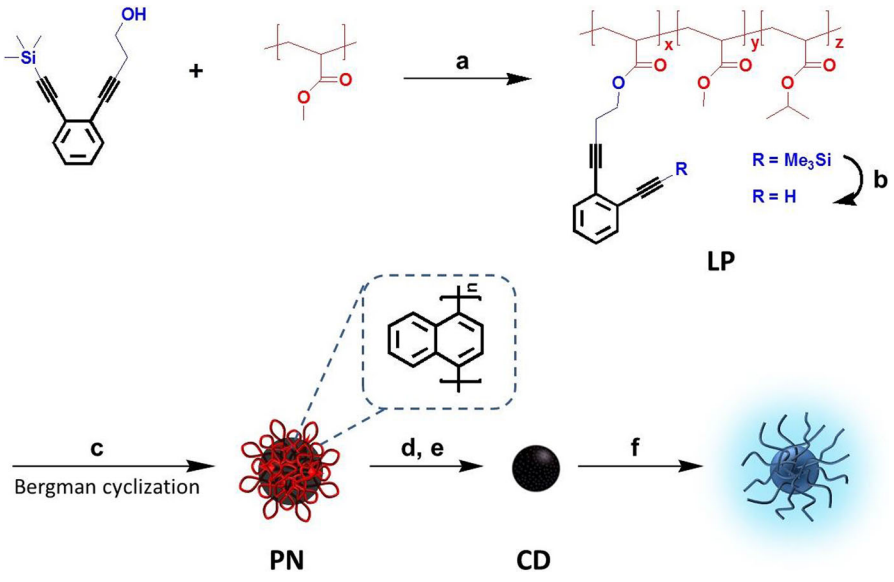

Fig. 15 Illustration of preparation of photoluminescent carbon nanodots. **a** $Ti(OiPr)_4$, diphenylmethane, 120 °C, 24 h. **b** TBAF, *p*-toluenesulfonic acid, tetrahydrofuran, RT, 2 h. **c** Diphenyl ether, reflux, 6 h. **d** 500 °C, 30 min. **e** 5 M HNO_3, reflux, 12 h. **f** PEG_{2000N}, H_2O, reflux, 72 h [55]

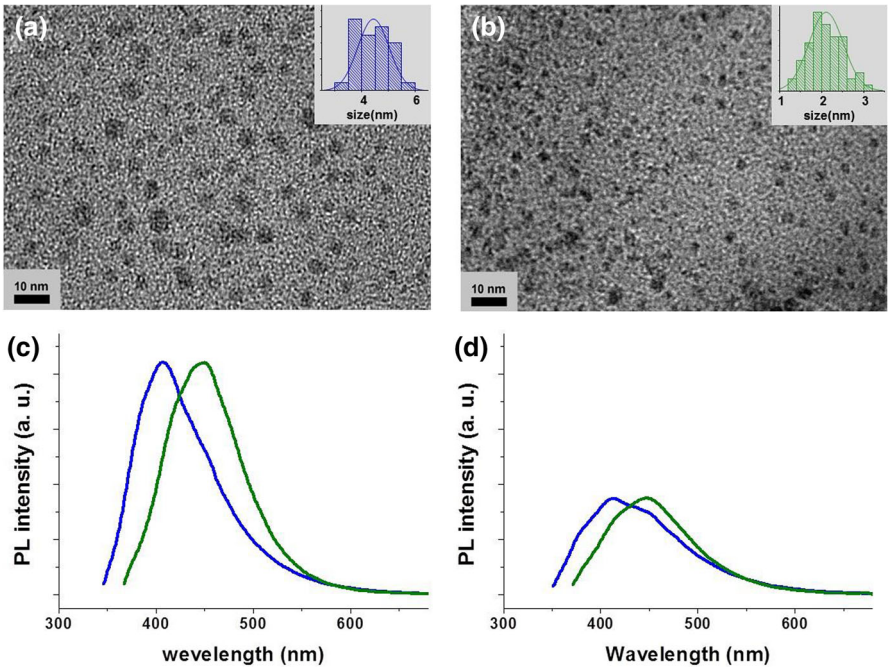

Fig. 16 Sizes and size-dependent PL spectra of C-dots. **a** TEM image and size histogram (*inset*) of CD-1. **b** TEM image and size histogram (*inset*) of CD-2. **c** PL spectra of surface-oxidized CD-1 (*blue line*) and CD-2 (*green line*) excited at 340 nm. **d** PL spectra of surface-reduced CD-1 (*blue line*) and CD-2 (*green line*) excited at 340 nm. Reproduced from [55] with permission from RSC

and the PL solely originated from e–h pair recombination in localized sp^2 carbon clusters, which are composed of two entirely different classes of carbon: crystalline and amorphous. The PL mechanism of C-dots formed from these two different sources was studied theoretically using density functional theory by choosing fused aromatic rings and cyclo-1,4-naphthylenes as model compounds (Fig. 17). For C-dots with graphitized carbon core, the energy gap between the highest occupied molecular orbital (HOMO) and lowest unoccupied molecular orbital (LUMO) decreases with increasing size of these sp^2 clusters. For C-dots with disordered carbon core, however, the smaller size of the CNs releases more strain energy in the excited state, resulting in a narrower energy gap.

The SCNPs were also used as size-tunable nanoreactors to fabricate and encapsulate inorganic quantum dots (QDs) in a one-pot reaction [56]. Poly(benzyl acrylate) (PBzA) nanoparticles were prepared by the same method mentioned above, followed by hydrogenolysis on Pd/C to obtain hydrophilic poly(acrylic acid) (PAA)-based nanoreactors. The carboxy groups in these nanoreactors can interact with zinc ions and trap them internally, allowing their subsequent reaction with S^{2-} to obtain ZnS QDs in situ (Fig. 18). As shown in Fig. 19, almost spherical QDs with average diameter of 4.1 nm were well dispersed on the copper grid. Larger PAA nanoparticles led to ZnS QDs of similar size and emission wavelength, but decreased QYs from QDs@PN1 to QDs@PN3 (17, 6, and 2 %). The latter result is

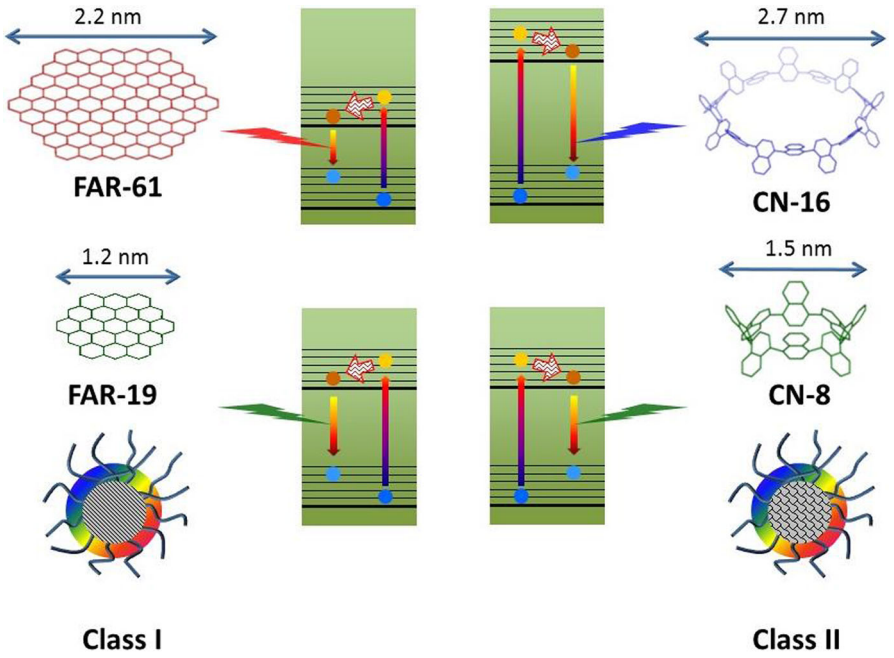

Fig. 17 Schematic illustration of PL mechanism of C-dots. The number after fused aromatic rings (FARs) indicates the number of hexagonal rings. The number after cyclo-1,4-naphthylene (CN) indicates the number of repeating units. Reproduced from [55] with permission from RSC

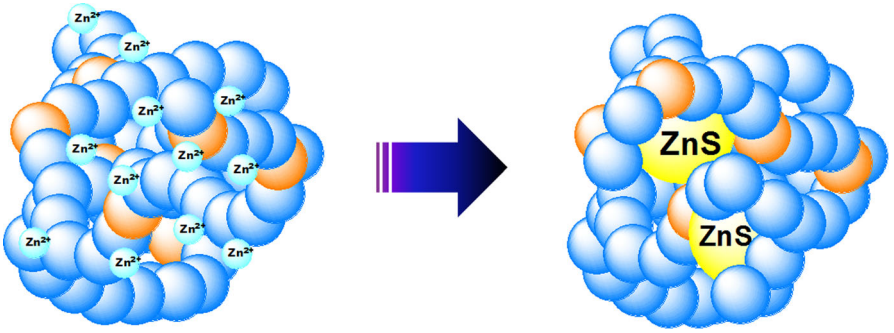

Fig. 18 Fabrication of ZnS nanocrystals in polymeric nanoreactors [56]

probably due to the fact that PAA nanoparticles of larger size can hold too many ZnS QDs, decreasing the distance between neighboring QDs and resulting in fluorescence quenching. Nevertheless, CdS QDs@PN1 exhibited bright fluorescence centered at 450 nm, with calculated QY of 45 % and average QD diameter of about 4.7 nm.

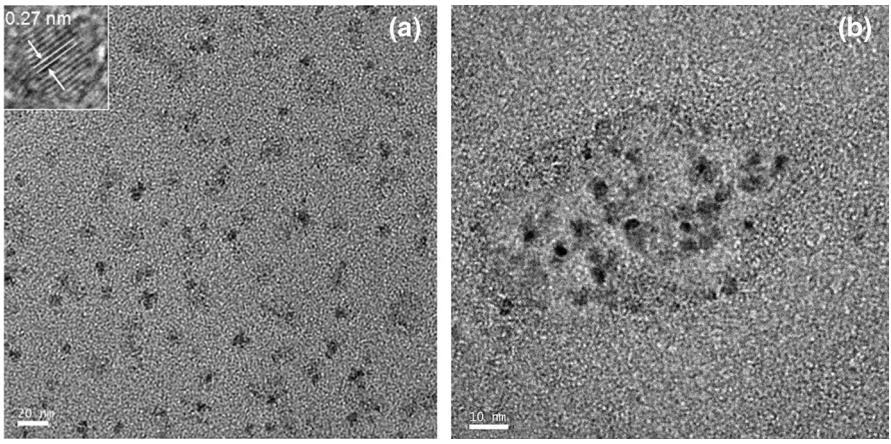

Fig. 19 TEM images of ZnS nanocrystals in polymeric nanoreactors. **a** QDs@PN1 (*inset* shows high-resolution image of lattice structure of ZnS), *scale bar* 20 nm. **b** QDs@PN3, *scale bar* 10 nm. Reproduced from [56] with permission from Wiley–VCH

4 Fabrication of Polymeric Nanomembranes

Polymer nanomembranes are receiving increasing attention due to their ultrathin nanostructure, just like other two-dimensional (2D) nanomaterials. Gölzhäuser et al. obtained free-standing polymer nanomembranes with controlled thickness and porosity via radiation-induced crosslinking of aromatic self-assembled monolayers (SAMs) [57]. However, only plate-like nanomembranes can be prepared due to the straight nature of electron motion. Polymer nanomembranes with various morphologies can be obtained via cross-coupling reaction of alkynyl SAMs on various templates [58], but a metal-containing catalyst was required for this process. Bergman cyclization is a wet chemical strategy with an in situ reaction mechanism that can be used to construct polymer nanomembranes with various morphologies inherited from the templates. The resulting polymer nanomembranes can also be carbonized to obtain carbon nanomembranes (CNMs). The overall procedure, shown in Fig. 20, includes: (1) formation of enediyne SMAs on various templates, (2) Bergman cyclization to obtain polymer nanomembranes, (3) carbonization to obtain CNM–template composites, and (4) template removal to obtain free-standing CNMs.

Initial work was performed by installing a tethering group on the enediyne moiety and immobilizing this compound onto the surface of mesoporous silica (SBA-15) as substrate to construct tubular carbon monolayers [59]. After formation of enediyne SAMs on activated SBA-15, Bergman cyclization of these surface-bound enediynes was performed in a medium heated at 260 °C under vacuum, yielding networks of PNs. Successive carbonization at 750 °C was carried out to remove volatile components, following which the SBA-15 template was etched off using aqueous HF. Finally, the powder was heated under vacuum at 900 °C to obtain ultrathin carbon nanotubes. The TEM images shown in Fig. 21 imply

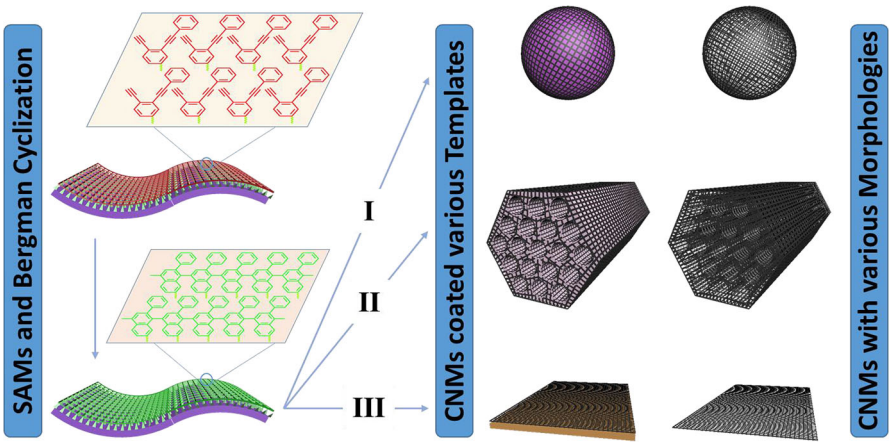

Fig. 20 Preparation of CNMs through Bergman cyclization of self-assembly monolayer (SAM) of EDY on templates with various microstructures and subsequent carbonization (and template removal). After SAM formation on various templates and Bergman cyclization, CNM-coated templates can be prepared via carbonization and free CNMs with various morphologies can be obtained after template removal

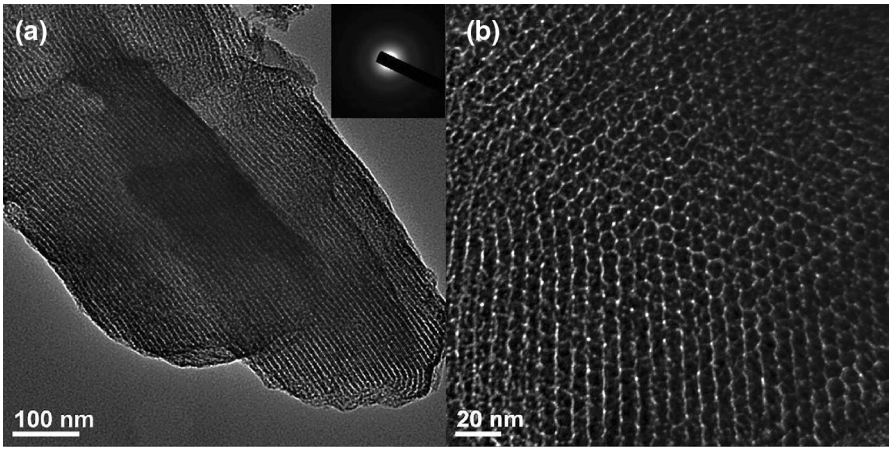

Fig. 21 TEM images viewed along [110] (**a**) and [001] (**b**) directions, with SAED pattern (*inset*) of tubular carbon monolayer. Reproduced from [59] with permission from ACS

successful replication of the SBA-15 template. Two well-separated rings were observed in the selected-area electron diffraction pattern of this carbonaceous material, which correlated to the respective major indices [100] and [110] of graphite nanostructures. In addition, by changing the template, this work was extended to synthesis of ordered porous carbon [60] (Fig. 22a), carbon nanoplates (Fig. 22b), and coating of Fe_3O_4 nanoparticles [61].

Further modification of the carbon thin film-lined SBA-15 to embed Pd nanoparticles inside the nanotubes resulted in new size-tunable nanoreactors for catalytic applications (Fig. 23a) [62]. Pd@SBA-15© (eventually renamed as SS-

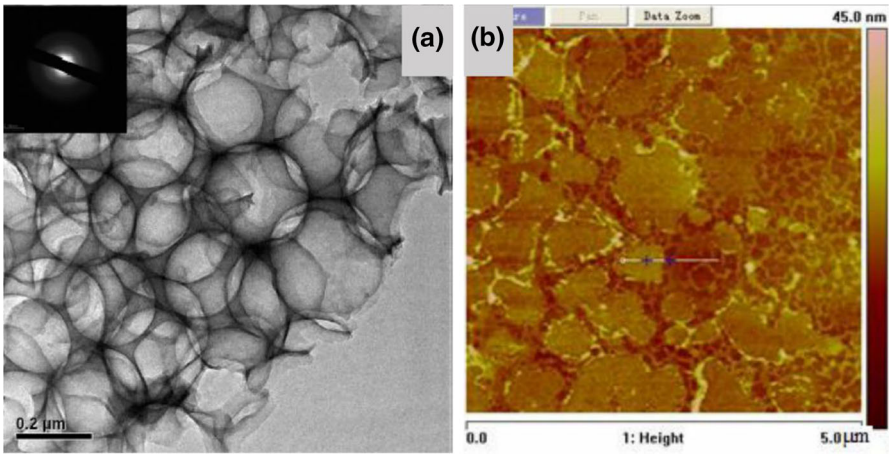

Fig. 22 **a** TEM image of ordered porous CNMs and **b** AFM image of plate-like CNMs. Reproduced from [60] with permission from ACS

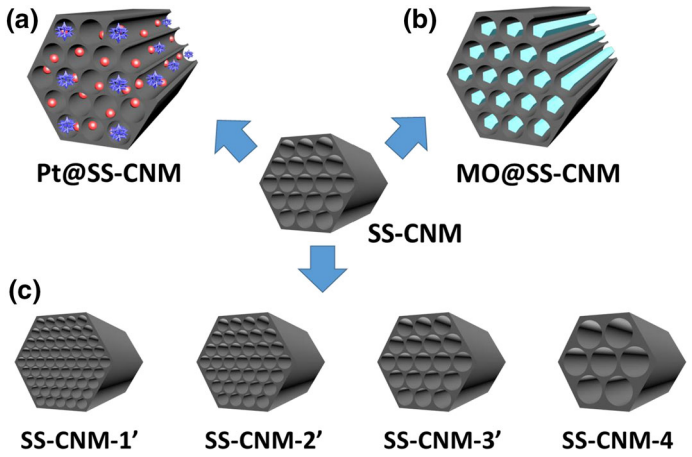

Fig. 23 Applications of tubular SS-CNMs in supercapacitors and catalysis in our group. **a** Pd nanoparticle-embedded SS-CNM as nanoreactor for coupling reactions. **b** Metal oxide-embedded SS-CNM to improve the capacitance and stability of supercapacitors. **c** Tunable pore sizes to study the relationship between electrical capacitance and pore size

CNM) nanoreactors with Pd content of 3.5 % were prepared by wetness impregnation technique with H_2PdCl_4 followed by reduction of Pd(II) to Pd(0) under hydrogen atmosphere. This nanoreactor revealed highly efficient heterogeneous Suzuki–Miyaura cross-coupling reactions in aqueous media, and could be easily separated and recovered from the reaction mixture. The catalytic activity did not deteriorate even after reuse several times, indicating enhanced stability of the nanoreactors mainly benefiting from the carbon thin-film lining. Kinetic study showed that, with addition of naphthalene or anthracene, the coupling reactions

were significantly decelerated, whereas addition of decalin slowed down the reaction only slightly, further confirming that the carbon film was essential to ensure good reactivity of the catalyst due to its hydrophobic environment (as aromatic compounds can coordinate with the graphene layer of a carbonaceous surface through π–π interactions).

Exploration of this newly designed nanoreactor in the synthesis of soluble conjugated microporous polymers (SCMPs) offered exciting results (Fig. 24) [63]. Preparation of conjugated microporous polymers through hyperbranching polycondensation is generally hard to control, and usually leads to insoluble polymer networks regardless of the solvent used. To solve the solubility problem, we limited the Suzuki-type polycondensation to exclusively take place inside Pd@SS-CNM nanoreactors, and successfully synthesized size-controlled SCMPs. In this study, three silica-supported carbon nanomembranes (denoted as SS-CNM-1, SS-CNM-2, and SS-CNM-3) with pore size of 3.4, 5.4, and 7.2 nm were prepared from MCM-41, SBA-15, and pore-expanded SBA-15, respectively. TEM images showed that all the palladium nanoparticles were well dispersed inside the channels with no palladium nanoparticles found outside the nanoreactors, which is essential for confined growth of SCMPs. Polycondensations performed in DMF with Pd@SS-CNM as catalyst and tetrabutylammonium fluoride (TBAF) as base produced three series of narrowly dispersed SCMPs (SCMP1, SCMP2, and SCMP3) with average size of 2.4, 3.8, and 5.4 nm, respectively (Fig. 25), only slightly smaller than the pore sizes of the nanoreactors, thus implying that the size of the SCMPs was controlled by the pore size of the nanoreactors, because the polycondensations took place exclusively inside the confined pores of the SS-CNM nanoreactors. Based on theoretical simulations, the calculated sizes of generation 2, 3, and 4 dendrimers correspond quite well with the experimental values of SCMP1, SCMP2, and SCMP3, respectively. More interestingly, the smallest SCMPs (SCMP1) could diffuse into the mesochannels of the larger nanoreactors (SS-CNM-2 and SS-CNM-3) to further get their terminal groups functionalized with iodobenzene. In contrast, the medium-sized SCMP nanoparticles could only enter the largest nanoreactors, whereas the largest SCMP nanoparticles were hardly able to enter any of the nanoreactors, leading to negligible consumption of iodobenzene as monitored by gas chromatography. This set of experiments unambiguously demonstrated that the polycondensation constitutes truly confined growth with the monomers accessing the palladium nanoparticles through the open channels. This catalyst@pore strategy can also be generally appreciated for synthesis of other types of soluble

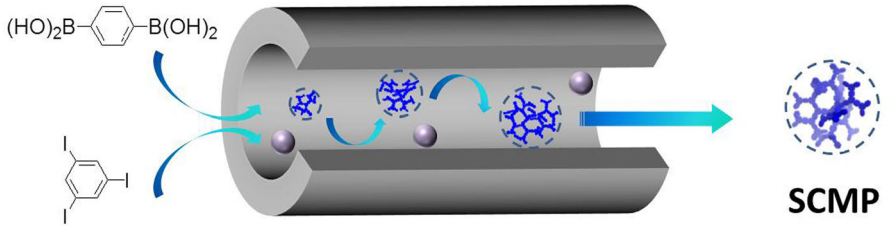

Fig. 24 Size-controlled synthesis of SCMPs in nanoreactors [63]

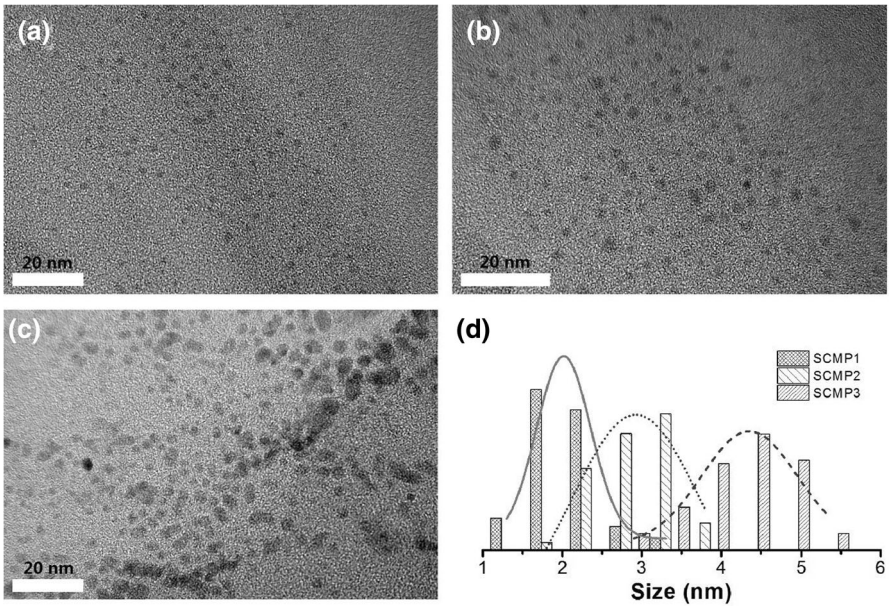

Fig. 25 High-resolution (HR)-TEM images of SCMP1 (**a**), SCMP2 (**b**), and SCMP3 (**c**). **d** Size histogram of three SCMPs obtained by HR-TEM [63]

hyperbranched polymers by using different types of monomer, with the size of the different kinds of SCMP being exactly controlled by the nanoreactors. In addition, such controllable preparation of SCMPs has also been extended to a heterogeneous catalysis system [64]. The combination of physical stability and processability offered by SCMPs makes them particularly attractive for use in polymer light-emitting diodes (PLEDs) and polymer solar cells.

Use as electrodes of supercapacitors is another important application of SS-CNMs. The SS-CNM can act as a host electrode material due to its high surface area, tunable structure, and good conductivity, whereas Co_3O_4 nanoparticles were used as the electronically active component (Fig. 23b) [65]. A series of Co_3O_4@SS-CNM composites with different Co_3O_4 content (24, 50, 66, and 80 wt%) were synthesized by facile wetness impregnation method with $Co(NO_3)_2$ as precursor followed by oxidation in air. In particular, Co_3O_4(66 %)@SS-CNM exhibited the highest specific capacitance, probably due to improved dispersion of Co_3O_4 which improved the electronic transmission inside the channels and further increased both the electrical conductivity of the composites and the electrochemical utilization of the pristine Co_3O_4 during the charge/discharge process. This supercapacitor electrode material exhibited maximum specific capacitance of 1086 F/g (1645 F/g based on Co_3O_4) in 6 M KOH solution. After 10,000 cycles, retention of 90 % of the initial capacitance was observed, indicating excellent electrochemical stability of the electrode. This strategy can be freely extended to incorporate other electroactive metal oxides in SS-CNMs to fabricate high-performance electrode materials for supercapacitors [66].

The complex relationship between the textural parameters of the electrode material and the supercapacitance of electrochemical capacitors (ECs) was studied by fabricating four SS-CNMs with similar geometry but different mesopore size [67]. SS-CNM-1′, SS-CNM-2′, and SS-CNM-3′ were obtained by the same methods mentioned above, whereas SS-CNM-4 was prepared from another expanded SBA-15 as shown in Fig. 23c. The pore sizes of these SS-CNMs were determined with the Brunauer–Emmett–Teller (BET) equation to be 3.05 nm, 4.14 nm, 6.68 nm, and 8.02 nm, respectively. All the samples produced quasirectangular CV curves along the current–potential axis (Fig. 26a), indicating ideal capacitive behavior. Furthermore, the galvanostatic charge–discharge curves were linear and symmetrical (Fig. 26b), which is a typical characteristic of an ideal EDL capacitor. Moreover, it is notable that high specific capacitance of 305 F/g was obtained for SS-CNM-2′ at 10 mV/s, superior to the values of 68, 173, and 75 F/g obtained for the SS-CNM-1′, SS-CNM-3′, and SS-CNM-4 composites, respectively. Theoretical modeling further validated this curved dependence of the supercapacitance on the pore size of the mesoporous electrode material, leading to the conclusion that optimal capacitance of ECs can be achieved using porous carbon electrode material with open pores of 3.0–5.0 nm (Fig. 27).

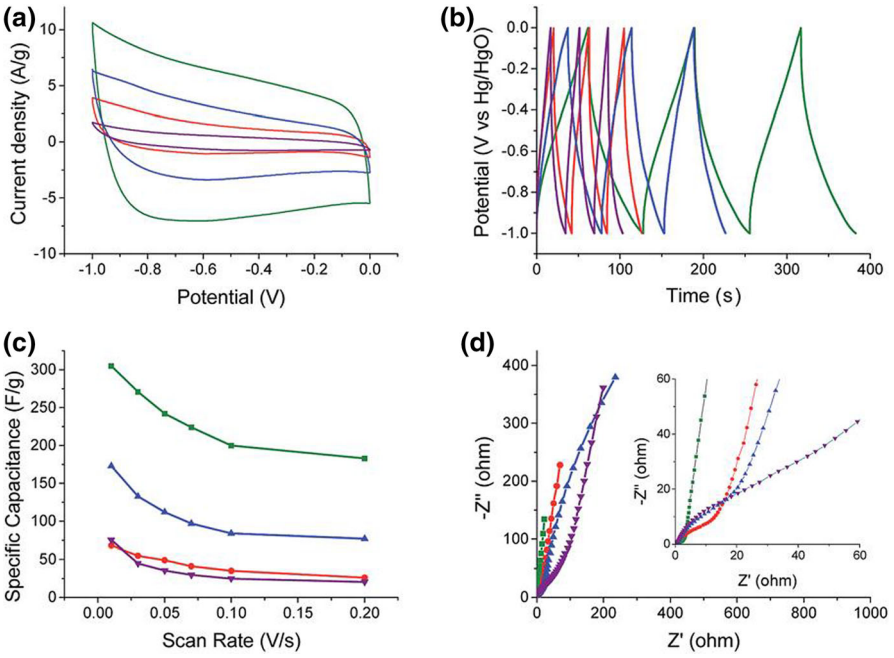

Fig. 26 Electrochemical evaluation of SS-CNM electrode materials (SS-CNM-1′ *red*; SS-CNM-2′ *green*; SS-CNM-3′ *blue*; SS-CNM-4 *purple*) using aqueous electrolyte of 6.0 M potassium hydroxide (KOH) dissolved in deionized water. **a** CV curves of four SS-CNM electrode materials obtained at scan rate of 0.05 V/s. **b** Galvanostatic charge–discharge curves of SS-CNM electrode materials when operated at current density of 5 A/g. **c** Stack capacitance values calculated from CV curves as function of scan rate. **d** Impedance Nyquist plots of the SS-CNMs. Reproduced from [67] with permission from RSC

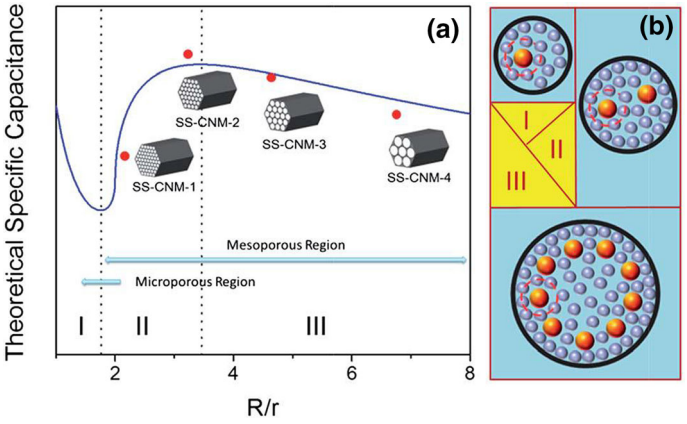

Fig. 27 **a** Fitting the specific capacitances of the SS-CNMs with the model plot. **b** Drawings of solvated ions residing in pores with *R*/*r* values of 1.5 (*top left*), 2 (*top right*), and 4 (*bottom*). Reproduced from [67] with permission from RSC

5 New Challenges

Despite the progress in materials chemistry, limitations still exist for Bergman cyclization, especially with respect to the ill-defined structure of the main chain. Matzger et al. [33] proposed a mechanism combining radical chain growth with step-growth pathways during the polymerization process (Fig. 28), in which the enediyne is first attacked by radical A (formed from Bergman cyclization) at 1- or 2-position of the alkynyl group to form a vinyl radical intermediate (intermediate B or D). Subsequent 5-exo-dig cyclization of B and 5-endo-dig cyclization of D produce radicals with an indene moiety, whereas 6-endo-dig cyclization of B produces radical with a naphthalene moiety, thus leading to random copolymers of naphthalene and indenylenemethylene instead of polynaphthalene. This mixed mechanism limits further development of Bergman cyclization in the field of controllable synthesis of conjugated polymers. To solve this problem, a strategy involving closure of the reaction pathways of the step-growth mechanism is required, which however seems to be unattainable given the diradical nature of the reaction intermediate. This issue inspired our attempts to extend research into the mechanism of Bergman cyclization to develop a novel ionic cycloaromatization of enediynes.

The question of whether Bergman cyclization can be forced to proceed in a different way perplexed us for a long time, until Alabugin et al. [68, 69] proposed a diradical/zwitterion dichotomy in cycloaromatization reactions. Bergman cyclization is one of the cycloaromatization reactions which decouple two electrons by breaking two π-bonds to form only one σ-bond. Such unusual processes can either create a pair of radical centers or be polarized to form a zwitterion. Although the latter should be disfavored by the coulombic penalty for separating the charges and, in some cases, by the intrinsic instability of the aryl cations, there is increasing evidence that such possibilities are surprisingly abundant and thus the utility of

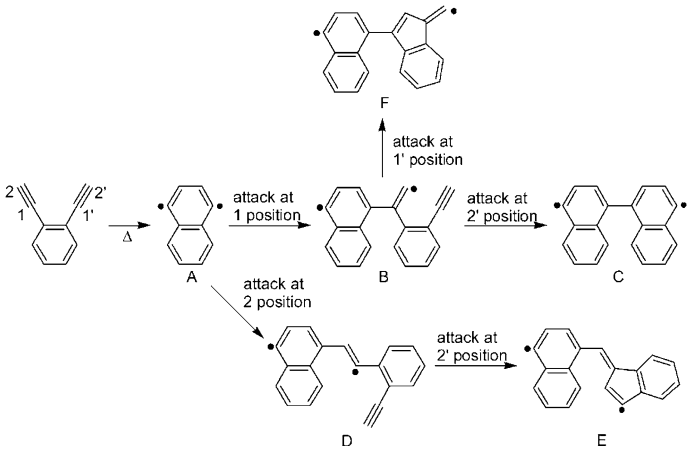

Fig. 28 Possible mechanism of Bergman cyclization [33]

cycloaromatization reactions can extend beyond radical chemistry to the preparation of zwitterions. In 2007, Perrin et al. [70] first disclosed that *p*-benzyne can interact with halide nucleophiles to produce *p*-substituted phenyl anions, which were subsequently trapped by protonation (Fig. 29). Kinetic analysis suggested that cyclization is the rate-limiting step but that the nucleophilic trapping also has a barrier, which has been attributed to solvation effects. The reactions of *p*-benzyne with anionic nucleophiles were calculated to be exergonic, in contrast to the reaction with a neutral nucleophile (e.g., H_2O). Hansmann et al. [71] later described a new reactivity pattern catalyzed by gold, in which two gold centers synchronously activate an enediyne system (dual activation). One gold center acted as a π Lewis acidic compound activating one of the alkynes, whereas the other gold center formed a gold acetylide, which then reacted as a nucleophile through the C_α or C_β atom. With 2,3-substituted thiophene-derived enediyne systems, the 6-endo cyclization initially led to a 1,3-diaurated species, which underwent a gold shift by an aryne-gold transition state to form a 1,4-diaurated species bearing a carbene moiety, followed by C–H insertion (Fig. 30). Other ionic cycloaromatization reactions of enediynes initiated by attack of an external anionic nucleophile or a nucleophilic group present in the molecule at the C≡C bond have also been discovered in the last decade [72], often providing derivatives of polynuclear heterocyclic molecules that are important from a biochemical point of view. All

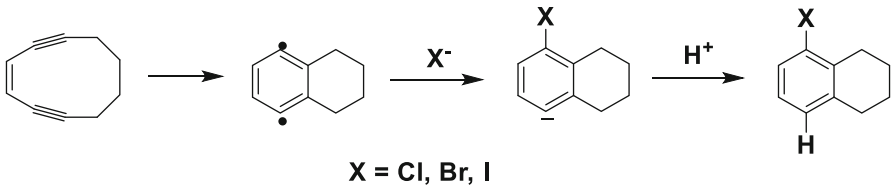

Fig. 29 Interaction of *p*-benzyne with halide anions illustrates the feasibility of zwitterionic cycloaromatization of enediynes [70]

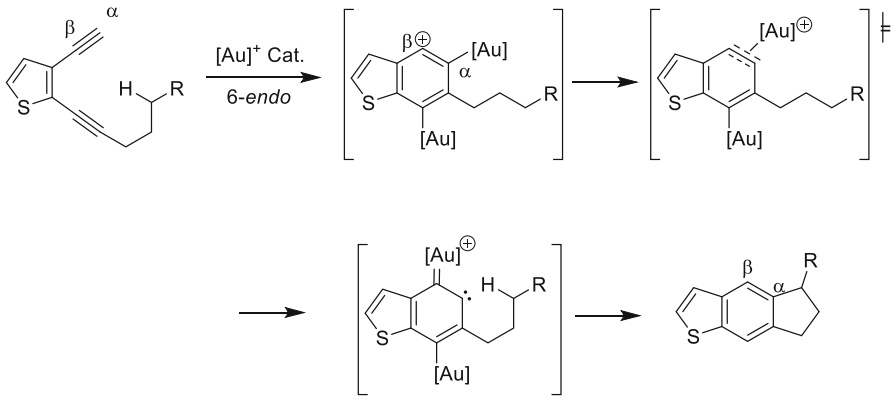

Fig. 30 Dual-gold-catalyzed cyclizations of enediynes [71]

these studies lay a mechanistic foundation for further development of this emerging field. We anticipate that, with subtle adjustment of the reaction conditions, substitution patterns, and catalysts, enediynes should be able to undergo ionic cycloaromatization to generate conjugated polymers. Very recently, we achieved cationic Bergman cyclization with strong acid as initiator, obtaining new conjugated polymers with high molecular weight and relatively narrow molecular weight distribution [73]. Future research involving Bergman cyclization will continue to uncover new fundamental factors controlling the chemical reactivity and contribute to the design of new functional materials.

6 Conclusions

Bergman cyclization has attracted increasing attention as an emerging and extraordinary strategy for preparation of aromatic polyarylenes and carbon-rich nanomaterials. Considerable efforts have been directed at understanding and expanding the various processes involved in synthesis of enediynes, polymerization strategies, and functionalization, and further conversion to carbon nano-allotropes. Recent years have witnessed broad achievements of Bergman cyclization in materials science, especially in developing new synthetic routes for carbon-rich nanoparticles/networks, carbon nanomembranes, and nanodevices. However, it is still at its infancy in this area with much room for improvement; For example, the PPPs formed from DNHD on Cu(110) surface cannot be converted to graphene nanoribbons directly (Fig. 2). One more example is that one can obtain graphene nanoplates using silicon as template, but it is challenging to grow large-scale graphene in this way (Fig. 22b). This may be because rapid chain transfer or termination of radicals causes unwanted five-membered cyclization to form "indene" structure defects [33], strongly hindering further growth of the nanographene. This mixed mechanism limits further development of Bergman cyclization in the field of controllable synthesis of conjugated polymers. To solve

this problem, closure of the reaction pathways of the step-growth mechanism is required, which however seems to be unattainable due to the diradical nature. This issue inspired our attempts to extend research into the mechanism of Bergman cyclization and develop a novel ionic cycloaromatization of enediynes. Therefore, much interest has been devoted to redirecting Bergman cyclization from the usual formation of a diradical towards a zwitterionic or ionic pathway, and polymerizations based on ionic cycloaromatization of enediynes are likely to be discovered in the near future.

Acknowledgements Financial support by the National Natural Science Foundation of China (21674035, 21474027, 91023008, 20874026, 20704013), Shanghai Shuguang Project (07SG33), New Century Excellent Talents in University, Ph.D. Programs Foundation of Ministry of Education of China, and Shanghai Leading Academic Discipline Project (B502) is gratefully acknowledged. A.H. thanks the Eastern Scholar Professorship and follow-up plan support from Shanghai local government. Y.W. thanks the China Scholarship Council (CSC) for support of his study at The University of Chicago.

References

1. Jones RR, Bergman RG (1972) *p*-Benzyne. Generation as an intermediate in a thermal isomerization reaction and trapping evidence for the 1,4-benzenediyl structure. J Am Chem Soc 94:660
2. Bergman RG (1973) Reactive 1,4-dehydroaromatics. Acc Chem Res 6:25
3. Lee MD, Dunne TS, Siegel MM, Chang CC, Morton GO, Borders DB (1987) Calichemicins, a novel family of antitumor antibiotics. 1. Chemistry and partial structure of calichemicin.gamma.1I. J Am Chem Soc 109:3464
4. Lee MD, Dunne TS, Chang CC, Ellestad GA, Siegel MM, Morton GO, McGahren WJ, Borders DB (1987) Calichemicins, a novel family of antitumor antibiotics. 2. Chemistry and structure of calichemicin.gamma.1I. J Am Chem Soc 109:3466
5. Konishi M, Ohkuma H, Tsuno T, Oki T, VanDuyne GD, Clardy J (1990) Crystal and molecular structure of dynemicin A: a novel 1,5-diyn-3-ene antitumor antibiotic. J Am Chem Soc 112:3715
6. Golik J, Clardy J, Dubay G, Groenewold G, Kawaguchi H, Konishi M, Krishnan B, Ohkuma H, Saitoh K, Doyle TW (1987) Esperamicins, a novel class of potent antitumor antibiotics. 2. Structure of esperamicin X. J Am Chem Soc 109:3461
7. Golik J, Dubay G, Groenewold G, Kawaguchi H, Konishi M, Krishnan B, Ohkuma H, Saitoh K, Doyle TW (1987) Esperamicins, a novel class of potent antitumor antibiotics. 3. Structures of esperamicins A1, A2, and A1b. J Am Chem Soc 109:3462
8. Leet JE, Schroeder DR, Hofstead SJ, Golik J, Colson KL, Huang S, Klohr SE, Doyle TW, Matson JA (1992) Kedarcidin, a new chromoprotein antitumor antibiotic: structure elucidation of kedarcidin chromophore. J Am Chem Soc 114:7946
9. Biggins JB, Onwueme KC, Thorson JS (2003) Resistance to enediyne antitumor antibiotics by calC self-sacrifice. Science 301:1537
10. Basak A, Mandal S, Bag SS (2003) Chelation-controlled Bergman cyclization: synthesis and reactivity of enediynyl ligands. Chem Rev 103:4077
11. Kar M, Basak A (2007) Design, synthesis, and biological activity of unnatural enediynes and related analogues equipped with pH-dependent or phototriggering devices. Chem Rev 107:2861
12. Hatial I, Jana S, Bisai S, Das M, Ghosh AK, Anoop A, Basak A (2014) Trienediynes on a 1,3,5-trisubstituted benzene template: a new approach for enhancement of reactivity. RSC Adv 4:28041
13. Kraka E, Cremer D (2014) Enediynes, enyne-allenes, their reactions, and beyond. Wiley Interdiscip Rev 4:285
14. Nicolaou KC, Ogawa Y, Zuccarello G, Schweiger EJ, Kumazawa T (1988) Cyclic conjugated enediynes related to calicheamicins and esperamicins: calculations, synthesis, and properties. J Am Chem Soc 110:4866
15. Magnus P, Fortt S, Pitterna T, Snyder JP (1990) Synthetic and mechanistic studies on esperamicin A1 and calichemicin.gamma.1. Molecular strain rather than.pi.-bond proximity determines the cycloaromatization rates of bicyclo[7.3.1]enediynes. J Am Chem Soc 112:4986

16. Snyder JP (1990) Monocyclic enediyne collapse to 1,4-diyl biradicals: a pathway under strain control. J Am Chem Soc 112:5367
17. Klein M, Walenzyk T, Konig B (2004) Electronic effects on the Bergman cyclisation of enediynes. A review. Collect Czech Chem Commun 69:945
18. Warner BP, Millar SP, Broene RD, Buchwald SL (1995) Controlled acceleration and inhibition of Bergman cyclization by metal chlorides. Science 269:814
19. Kaya K, Johnson M, Alabugin IV (2015) Opening enediyne scissors wider: pH-dependent dna photocleavage by meta-diyne lysine conjugates. Photochem Photobiol 91:748
20. Campolo D, Arif T, Borie C, Mouysset D, Vanthuyne N, Naubron JV, Bertrand MP, Nechab M (2014) Double transfer of chirality in organocopper-mediated bis(alkylating) cycloisomerization of enediynes. Angew Chem Int Ed 53:3227
21. Nösel P, Müller V, Mader S, Moghimi S, Rudolph M, Braun I, Rominger F, Hashmi ASK (2015) Gold-catalyzed hydroarylating cyclization of 1,2-bis(2-iodoethynyl)benzenes. Adv Synth Catal 357:500
22. John JA, Tour JM (1994) Synthesis of polyphenylenes and polynaphthalenes by thermolysis of enediynes and dialkynylbenzenes. J Am Chem Soc 116:5011
23. Rettenbacher AS, Perpall MW, Echegoyen L, Hudson J, Smith DW (2007) Radical addition of a conjugated polymer to multilayer fullerenes (carbon nano-onions). Chem Mater 19:1411
24. Smith DW, Shah HV, Perera KPU, Perpall MW, Babb DA, Martin SJ (2007) Polyarylene networks via Bergman cyclopolymerization of bis-ortho-diynyl arenes. Adv Funct Mater 17:1237
25. Rule JD, Wilson SR, Moore JS (2003) Radical polymerization initiated by Bergman cyclization. J Am Chem Soc 125:12992
26. Rule JD, Moore JS (2005) Polymerizations initiated by diradicals from cycloaromatization reactions. Macromolecules 38:7266
27. Gerstel P, Barner-Kowollik C (2011) RAFT mediated polymerization of methyl methacrylate initiated by Bergman cyclization: access to high molecular weight narrow polydispersity polymers. Macromol Rapid Commun 32:444
28. Xiao Y, Hu A (2011) Bergman cyclization in polymer chemistry and material science. Macromol Rapid Commun 32:1688
29. Tour JM (1994) Soluble oligo- and polyphenylenes. Adv Mater 6:190
30. Sun Q, Zhang C, Li Z, Kong H, Tan Q, Hu A, Xu W (2013) On-surface formation of one-dimensional polyphenylene through Bergman cyclization. J Am Chem Soc 135:8448
31. Sun S, Dong L, Song D, Huang B, Hu A (2015) Synthesis of polyphenylenes through Bergman cyclization of enediynes with long chain alkyl groups. Chin J Polym Sci 33:184
32. Cheng X, Ma J, Zhi J, Yang X, Hu A (2010) Synthesis of novel "rod-coil" brush polymers with conjugated backbones through Bergman cyclization. Macromolecules 43:909
33. Johnson JP, Bringley DA, Wilson EE, Lewis KD, Beck LW, Matzger AJ (2003) Comparison of "polynaphthalenes" prepared by two mechanistically distinct routes. J Am Chem Soc 125:14708
34. Ma J, Ma X, Deng S, Li F, Hu A (2011) Synthesis of dendronized polymers through Bergman cyclization of enediyne-containing Frechet-type dendrimers. J Polym Sci Part A-Polym Chem 49:1368
35. Miao C, Zhi J, Sun S, Yang X, Hu A (2010) Formation of conjugated polynaphthalene via Bergman cyclization. J Polym Sci Polym Chem 48:2187
36. Sun S, Zhu C, Song D, Li F, Hu A (2014) Preparation of conjugated polyphenylenes from maleimide-based enediynes through thermal-triggered Bergman cyclization polymerization. Polym Chem 5:1241
37. Sun S, Huang B, Li F, Song D, Hu A (2015) Synthesis of chiral polyphenylenes through Bergman cyclization of enediynes with pendant chiral amino ester groups. Chin J Polym Sci 33:743
38. Ma J, Cheng X, Ma X, Deng S, Hu A (2010) Functionalization of multiwalled carbon nanotubes with polyesters via Bergman cyclization and "grafting from" strategy. J Polym Sci Part A-Polym Chem 48:5541
39. Ma J, Deng S, Cheng X, Wei W, Hu A (2011) Covalent surface functionalization of multiwalled carbon nanotubes through Bergman cyclization of enediyne-containing dendrimers. J Polym Sci Part A-Polym Chem 49:3951
40. Ma X, Li F, Wang Y, Hu A (2012) Functionalization of pristine graphene with conjugated polymers through diradical addition and propagation. Chem-Asian J 7:2547
41. Taranekar P, Park JY, Patton D, Fulghum T, Ramon GJ, Advincula R (2006) Conjugated polymer nanoparticles via intramolecular crosslinking of dendrimeric precursors. Adv Mater 18:2461

42. Tekade RK, Kumar PV, Jain NK (2009) Dendrimers in oncology: an expanding horizon. Chem Rev 109:49
43. Parrott MC, Benhabbour SR, Saab C, Lemon JA, Parker S, Valliant JF, Adronov A (2009) Synthesis, radiolabeling, and bio-imaging of high-generation polyester dendrimers. J Am Chem Soc 131:2906
44. Helms B, Meijer EW (2006) CHEMISTRY: dendrimers at work. Science 313:929
45. Mecerreyes D, Lee V, Hawker CJ, Hedrick JL, Wursch A, Volksen W, Magbitang T, Huang E, Miller RD (2001) A novel approach to functionalized nanoparticles: self-crosslinking of macromolecules in ultradilute solution. Adv Mater 13:204
46. Adkins CT, Muchalski H, Harth E (2009) Nanoparticles with individual site-isolated semiconducting polymers from intramolecular chain collapse processes. Macromolecules 42:5786
47. Moreno AJ, Lo Verso F, Sanchez-Sanchez A, Arbe A, Colmenero J, Pomposo JA (2013) Advantages of orthogonal folding of single polymer chains to soft nanoparticles. Macromolecules 46:9748
48. Mavila S, Eivgi O, Berkovich I, Lemcoff NG (2016) Intramolecular cross-linking methodologies for the synthesis of polymer nanoparticles. Chem Rev 116:878
49. Croce TA, Hamilton SK, Chen ML, Muchalski H, Harth E (2007) Alternative *o*-quinodimethane cross-linking precursors for intramolecular chain collapse nanoparticles. Macromolecules 40:6028
50. Ergin M, Kiskan B, Gacal B, Yagci Y (2007) Thermally curable polystyrene via click chemistry. Macromolecules 40:4724
51. Jiang XY, Pu HT, Wang P (2011) Polymer nanoparticles via intramolecular crosslinking of sulfonyl azide functionalized polymers. Polymer 52:3597
52. Hansell CF, Lu A, Patterson JP, O'Reilly RK (2014) Exploiting the tetrazine-norbornene reaction for single polymer chain collapse. Nanoscale 6:4102
53. Zhu B, Ma J, Li Z, Hou J, Cheng X, Qian G, Liu P, Hu A (2011) Formation of polymeric nanoparticles via Bergman cyclization mediated intramolecular chain collapse. J Mater Chem 21:2679
54. Zhu B, Qian G, Xiao Y, Deng S, Wang M, Hu A (2011) A convergence of photo-Bergman cyclization and intramolecular chain collapse towards polymeric nanoparticles. J Polym Sci Part A-Polym Chem 49:5330
55. Zhu B, Sun S, Wang Y, Deng S, Qian G, Wang M, Hu A (2013) Preparation of carbon nanodots from single chain polymeric nanoparticles and theoretical investigation of the photoluminescence mechanism. J Mater Chem C 1:580
56. Qian G, Zhu B, Wang Y, Deng S, Hu A (2012) Size-tunable polymeric nanoreactors for one-pot synthesis and encapsulation of quantum dots. Macromol Rapid Commun 33:1393
57. Turchanin A, Gölzhäuser A (2016) Carbon nanomembranes. Adv Mater 28:6075
58. Schultz MJ, Zhang X, Unarunotai S, Khang D-Y, Cao Q, Wang C, Lei C, MacLaren S, Soares JANT, Petrov I, Moore JS, Rogers JA (2008) Synthesis of linked carbon monolayers: films, balloons, tubes, and pleated sheets. PNAS 105:7353
59. Yang X, Li Z, Zhi J, Ma J, Hu A (2010) Synthesis of ultrathin mesoporous carbon through Bergman cyclization of enediyne self-assembled monolayers in SBA-15. Langmuir 26:11244
60. Li Z, Song D, Zhi J, Hu A (2011) Synthesis of ultrathin ordered porous carbon through Bergman cyclization of enediyne self-assembled monolayers on silica nanoparticles. J Phys Chem C 115:15829
61. Li Z, Zhu X, Chen S, Hu A (2013) Coating magnetite nanoparticles with a polyaryl monolayer through Bergman cyclization-mediated polymerization. Chem-Asian J 8:560
62. Zhi J, Song D, Li Z, Lei X, Hu A (2011) Palladium nanoparticles in carbon thin film-lined SBA-15 nanoreactors: efficient heterogeneous catalysts for Suzuki-Miyaura cross coupling reaction in aqueous media. Chem Commun 47:10707
63. Deng S, Zhi J, Zhang X, Wu Q, Ding Y, Hu A (2014) Size-controlled synthesis of conjugated polymer nanoparticles in confined nanoreactors. Angew Chem Int Ed 53:14144
64. Deng S, Zhao P, Dai Y, Huang B, Hu A (2015) Synthesis of soluble conjugated polymeric nanoparticles through heterogeneous Suzuki coupling reaction. Polymer 64:216
65. Zhi J, Deng S, Zhang Y, Wang Y, Hu A (2013) Embedding Co_3O_4 nanoparticles in SBA-15 supported carbon nanomembrane for advanced supercapacitor materials. J Mater Chem A 1:3171
66. Zhi J, Deng S, Wang Y, Hu A (2015) Highly ordered metal oxide nanorods inside mesoporous silica supported carbon nanomembranes: high performance electrode materials for symmetrical supercapacitor devices. J Phys Chem C 119:8530
67. Zhi J, Wang Y, Deng S, Hu A (2014) Study on the relation between pore size and supercapacitance in mesoporous carbon electrodes with silica-supported carbon nanomembranes. RSC Adv 4:40296

68. Mohamed RK, Peterson PW, Alabugin IV (2013) Concerted reactions that produce diradicals and zwitterions: electronic, steric, conformational, and kinetic control of cycloaromatization processes. Chem Rev 113:7089
69. Peterson PW, Mohamed RK, Alabugin IV (2013) How to lose a bond in two ways—the diradical/zwitterion dichotomy in cycloaromatization reactions. Eur J Org Chem 2013:2505–2527
70. Perrin CL, Rodgers BL, O'Connor JM (2007) Nucleophilic addition to ap-benzyne derived from an enediyne: a new mechanism for halide incorporation into biomolecules. J Am Chem Soc 129:4795
71. Hansmann MM, Tšupova S, Rudolph M, Rominger F, Hashmi ASK (2014) Gold-catalyzed cyclization of diynes: controlling the mode of 5-endo versus 6-endo cyclization—an experimental and theoretical study by utilizing diethynylthiophenes. Chem Eur J 20:2215
72. Gulevskaya AV, Tyaglivy AS (2012) Nucleophilic cyclizations of enediynes as a method for polynuclear heterocycle synthesis. Chem Heterocycl Compd 48:82
73. Chen S, Li Q, Sun S, Ding Y, Hu A (2017) A novel approach toward polyfulvene: cationic polymerization of enediynes. Macromolecules 50:534